

Highlights

- A mechanism for the limited shear-stress transition of an elastohydrodynamic lubrication (EHL) oil film is proposed.
- The spatial structure and velocity profile showed gradual changes.
- Suppression of the fluctuation is found in the EHL regime.

Molecular Origin of Limiting Shear Stress of Elastohydrodynamic Lubrication Oil Film Studied by Molecular Dynamics

Hitoshi Washizu^{a,b,c,*}, Toshihide Ohmori^a, Atsushi Suzuki^d

^a*Toyota Central R&D Labs., Inc., Nagakute, Aichi 480-1192, Japan*

^b*Graduate School of Simulation Studies, University of Hyogo 7-1-28
Minatojima-minamimachi, Chuo-ku, Kobe, Hyogo, Japan*

^c*Elements Strategy Initiative for Catalysts and Batteries, Kyoto University, Katsura, Kyoto
615-8520, Japan*

^d *AISIN AI Corporation, 1-33 Kounosu, Nishiazai-Cho, Nishio, Aichi, Japan*

Abstract

All-atom molecular dynamics simulations of an elastohydrodynamic lubrication oil film are performed to study the effect of pressure. Fluid molecules of n-hexane are confined between two solid plates under a constant normal force of 0.1–8.0 GPa. Traction simulations are performed by applying relative sliding motion to the solid plates. A transition in the traction behavior is observed around 0.5–2.0 GPa, which corresponds to the viscoelastic region to the plastic–elastic region, which are experimentally observed. This phase transition is related to the suppression of the fluctuation in molecular motion.

1. Introduction

Machine elements in which large loads are transmitted, such as a traction-drive continuously variable transmission (CVT), work in the elastohydrodynamic lubrication (EHL) regime [1]. The molecular dynamic behavior of the oil film for EHL is not well-understood since the long trajectories of ensembles of a large number of fluid molecules are required to analyze the drastic phase transition induced by a high pressure. Typical practical EHL conditions include a film thickness on the order of a submicron and a shear rate less than 10^6 /s for a submicron thick film [2]. Although this film thickness exceeds the range of van der Waals structural forces of the solid plates, the behavior of the fluid layer differs from that of the bulk, i.e., the traction coefficients (the tangential traction force divided by the normal load) cannot be easily deduced from the bulk shear viscosity.

In this letter, we report molecular dynamics (MD) simulations to study the effect of pressure. The hydrocarbon molecules are confined between two solid atom layers, and the pressure is added as a normal force to the solid atom layers. The solid atom layers move at a constant velocity so that shear is induced in the fluid film. Previous simulation of a submicron-thickness oil film showed

*Corresponding author

Email address: h@washizu.org (Hitoshi Washizu)

quantitative agreement between experiment and simulation [2, 3]. Here, we extend our study to examine the effect of an external pressure, in molecular level. In an EHL oil film, for an increasing external pressure, traction, i.e., the friction coefficient, saturates and does not depend on the shear rate at some pressure, which is called the limiting shear stress. Although this transition is assumed to have a relationship with glass transition from **liquid-like state to solid-like state**, the state of the fluid in EHL film is not the same as in a static condition of materials [4]. Moreover, the mechanism of the glass transition is under discussion, especially for hydrocarbons. For example, mode-coupling theory is a candidate for explaining the glass transition of particles, and the internal degrees of freedom coupled with the intermolecular interaction are very complex to model [5]. An all-atom non-equilibrium MD simulation is an effective tool to simulate the phase behavior under shear for understanding these phenomena. We use *n*-hexane fluid molecule as a typical hydrocarbon oil, in order to obtain a universality of the origin of limiting shear stress.

2. Method

All-atom MD simulations of a lubricating oil film confined between solid walls under shear conditions are executed using the following procedure. *n*-hexane is chosen as the fluid molecule so that the general behaviors of the hydrocarbon oils are simulated. The related sliding speed of the solid walls is set to $2v_{\text{wall}} = 1.0$ m/s, which is the usual driving condition in macroscopic machine elements such as a CVT.

In the MD simulation, the hydrocarbon molecules are dynamically treated using the AMBER force field [6]. On the x, y and z axes, periodic boundary conditions are adopted for the hexahedron simulation cell, where x is the sliding direction, and z is the direction of the fluid film thickness. The temperature is controlled at 350 K using the Nosé–Hoover thermostat [7]. All molecules are connected to a heat bath. While this has been shown to affect the rheology of the confined fluids at shear rates above $\dot{\gamma} = 0.2$ (in reduced Lennard–Jones units), the low shear rates here, a maximum of $\dot{\gamma}(\epsilon/mR^2)^{1/2} \approx 0.004$, suggest that such artifacts should be negligible [8, 9]. Each simulation step corresponds to 0.5 fs, and the time integral due to the motion of the atoms and molecules is calculated by the reversible reference system propagation algorithm (rRESPA) [10] method. The solid plate of an alpha-ferrous crystal is modeled as a solid atom layer with a lattice of $10 \times 10 \times 3$ in the x, y, z directions, and the lattice parameter is set to 2.87 Å. The fluid–solid interface is the (100) surface, and the vibrations of each solid atom are suppressed. The Lennard–Jones parameter for solid atoms is then set to 12.14 kcal/mol [2] in order to suppress boundary slip [3].

Constant shear states under a constant pressure and constant sliding velocity are obtained using the following procedure. A set of fluid molecules is first arranged in a lattice configuration. The molecules are then moved by the MD simulation under the periodic boundary conditions in the x, y , and z directions at a constant temperature of 350 K until a thermal equilibrium is obtained. Next, several sets of thermal equilibrium fluids are arranged in the z direction between two solid plates. Fluid molecules are compressed by the MD simulation under the periodic boundary conditions in the x and y directions by applying a constant pressure, p_{zz} , to the plates. The stress in the plates is in the z

direction. A shear in the x direction is then applied by the relative sliding motion of the Fe plates at the constant velocity, v_{wall} . The number of atoms is set to 576, which corresponds to a film thickness of 10 nm at 1 GPa to simulate a sufficiently thick oil film. If the oil film thickness is too small, the solid like behavior, such as stick-slip occur [2]. The film thickness is calculated from the average of the difference between the highest and lowest fluid molecules in the fluid film. The simulation code is parallelized and tested on a massively parallel computer, which was described in our previous work [2, 3].

3. Results and Discussion

The effect of the external pressure is studied by simulations of a 50-ns-long trajectory for each p_{zz} . Snapshot of the simulation of an n -hexane film in steady shear state with the relative sliding speed of $2v_{\text{wall}} = 1.0$ m/s, and at external pressure $p_{zz} = 8.0$ GPa, is shown in Fig. 1. The highly layered fluid molecules are found in the vicinity of the wall which is already reported in our previous work [2, 3]. In comparison with snapshots in other external pressures (they are shown in the graphical abstract), the film thickness is small and the density of the fluid molecules is high.

Figure 2a shows the external pressure dependence of the film thickness. The film thickness decreases monotonically with the increase in the external pressure. This tendency resembles that observed in experiments [11]. **In more detail, there would be a step decrease in the film thickness, which is shown for the liquid-solid transition in the bulk. In our simulation, however, finding the precise transition point is out of scope, since the system is under confinement and shear, we cannot compare with the experiment directly. The comparison of the static phase transition with the experiments in many kind of fluid molecules will be shown in the our next paper.** Figure 2b shows the external pressure dependence of the traction coefficient. The traction coefficient is calculated from the average force acting on both solid sheets divided by the external pressure p_{zz} . The traction coefficient first increases monotonically with the increase in the external pressure and plateaus when $p_{zz} \geq 1.0$ GPa. Although the shear rate differs in our simulation since the number of molecules is fixed so that the film thickness decreases owing to the increase in the external pressure, the simulation results show saturation of the shear stress. The limiting shear stress observed in the experiments is reproduced in the simulation, and a transition in the change in the traction coefficients is observed around $p_{zz} = 0.5$ – 1.0 GPa. This pressure regime may correspond to the melting pressure of n -hexane at 350K [12]. Although the range of critical p_{zz} almost corresponds to the experimental range, the critical traction coefficient cannot predicted quantitatively since the film thickness is very different under the experimental conditions and simulation conditions [2]. Therefore, we discuss the origin of the limiting shear stress qualitatively in the following.

From the experiments, this transition corresponds to a phase transition from the viscoelastic region to the plastic-elastic region [4]. In order to analyze the molecular mechanism of the phase transition, radial distribution functions (RDFs) are suitable for describing the static structural change in the ensemble of fluid molecules. Figure 3 shows the RDFs of the carbon atoms in the fluid molecules at the center of the fluid film. The molecules are chosen such that they are located 25% to 75% of the distance between plates. Note that the

first and second peaks correspond to the peaks between atoms in their own molecules. The outer region ($r > 0.3$ nm) shows the peaks in the intermolecular distribution of carbon atoms. In the RDFs, liquid-like distributions that have a single peak or two peaks in the outer region are found at a low pressure of $p_{zz} = 0.1\text{--}0.5$ GPa. As the pressure increases, the sharpness of the peaks in the outer region increases, and shifts in the peaks are observed. This is due to the increase in the density of the oil film. In other words, a decrease in the free volume of hydrocarbon molecules occurs, and the internal bond length between each internal atom is preserved within the simulated range of external pressures. From the viewpoint of the phase transition, however, the change in the RDFs is gradual, and an obvious transition in the curves around $p_{zz} = 1.0$ GPa is not observed. This means that the transition is not only related to the arrangement of the molecules.

In order to discuss the dynamic motion of the molecules, the velocity profiles at a low pressure ($p_{zz} = 0.5$ GPa), high pressure ($p_{zz} = 2.0$ GPa), and very high pressure ($p_{zz} = 8.0$ GPa) are plotted in Fig. 4a. v_x, v_y , and v_z are the velocities in the x, y , and z directions, respectively, and $\langle \rangle$ denotes the time average. At every external pressure p_{zz} , $\langle v_y \rangle$ and $\langle v_z \rangle$ are very low owing to the conservation of momentum. The small oscillation of $\langle v_z \rangle$ observed in the vicinity of both walls may due to the structuring of the fluid molecules [2, 3]. The velocity profiles for $\langle v_x \rangle$ differ for the external pressures. Newtonian-like profiles are observed at a low pressure, whereas non-Newtonian profiles are observed more strongly at higher pressures, which suggests an increase in the elastic interactions between molecules. The difference, however, is too small to explain the dramatic change in the traction behavior.

The differences in the molecular motion at low and high pressures are clearly shown in the profiles of the velocity fluctuation, which are shown in Fig. 4b. At a low pressure of $p_{zz}=0.5$ GPa, the degree of fluctuation in the velocity is three times larger than that at a high pressure. Moreover, plateau regions, i.e. regions in which the fluctuation curves are saturated are observed at the center of the oil film. This means that the effect of the wall is in a limited region from the wall, and the motions of the molecules do not depend on the film thickness. The $(v_x - \langle v_x \rangle)^2$ and $(v_y - \langle v_y \rangle)^2$ curves are almost identical and exhibit larger values than the $(v_z - \langle v_z \rangle)^2$ curves. This means that the fluctuations in the molecules are suppressed stronger in the z direction than in the x, y directions owing to the system confinement. Thus, the molecules can change positions in either the x or y directions, which is described by the Eyring viscosity [13].

At high pressures of $p_{zz}=2.0$ and 8.0 GPa, a plateau region is not observed, which indicates that the effect of the wall, reaches the center of the film in EHL regime. This is not because the local pressure at the center of the film changes as the normal pressure increases. The region of the correlation, such as the momentum correlation length in our previous paper [3], which is more than 50 nm under $p_{zz}=1.0$ GPa, has changed due to the increase of the external pressure. Here, the curves of $(v_y - \langle v_y \rangle)^2$ and $(v_z - \langle v_z \rangle)^2$ are identical. This means that fluctuation in the y direction is suppressed, as in z direction, so that the molecules are caught at fixed positions. In the x direction, the shear field causes a larger fluctuation than in the other directions. The bump shown in the curve of $(v_x - \langle v_x \rangle)^2$ at $p_{zz} = 8.0$ GPa may be related to the larger shear field at the center of the oil film. This suggests that the plasticity is related to the suppression of fluctuation in the molecular motion.

This tendency is also observed from an analysis of the segment (bond) motions. In Fig. 5, the autocorrelation functions $P_1(t) = \langle s(t) \cdot s(0) \rangle = \langle \cos(\theta(t)) \rangle$ of each segment of the *n*-hexane molecules \mathbf{s} are plotted for the ensemble of molecules in the vicinity of the solid walls and at the center of the fluid layers at a low pressure of $p_{zz} = 0.5$ GPa and high pressures of $p_{zz} = 2.0$ and 8.0 GPa. Here, $s(t)$ is a unit vector of \mathbf{s} , and $\theta(t)$ is the angle between \mathbf{s} at times t_0 and $t_0 + t$. Long-time tails of the correlation functions are observed in the vicinity of the walls. The relaxation times of the segment motions calculated from fitting the curves at the center of the fluid are 312, 2,294, and 3,846 ps at $p_{zz} = 0.5, 2.0$, and 8.0 GPa, respectively. At the wall, the relaxation times are 1,245, 10,913, and 23,161 ps at $p_{zz} = 0.5, 2.0$, and 8.0 GPa, respectively. The longer relaxation times observed for higher pressures at the center of the films are consistent with the explanation of the velocity fluctuation in Fig. 4b. At high pressures of $p_{zz} = 2.0$ and 8.0 GPa, the shear field does not induce a relative positional change in the molecular structure in the y and z directions so that the correlations between the bonds are almost fixed not only in the vicinity of the walls but at the center of the film.

The MD simulations have demonstrated that the EHL transition is not clearly observed from the change in the static liquid structure to the solid-like structure shown in Fig. 3. The dynamics of the average velocity in Fig. 4a show slight differences. A change is clearly observed for the velocity fluctuation in Fig. 4b. The velocity fluctuation is suppressed by a factor of more than three at a high pressure, and the bulk region of the velocity fluctuation disappeared. This change is also shown from the analysis of the segment motions in Fig. 5.

We have not taken into consideration of occurrence of shear bands [4], which is one of the explanation to the internal slip hypothesis for pressure independent shear stress. However, we have already obtained some characteristic features of the limiting shear stress in EHL film. From the continuous velocity profile in Fig. 4a, the shear localization or slip, which is related to the shear band is not found. In our simulation, the saturation of the traction coefficient is related to the bump of the velocity fluctuation at the center of the fluid film, which is shown in the v_x curve of $p_{zz} = 8.0$ GPa in Fig. 4b. The excess shear force may be canceled by the increase of the fluctuation in x direction at the center. The relation between our mechanism and experimentally observed shear bands would be explained in the long time simulation in realistic oil film thickness.

In our simulation, the temperature is set to a constant value of 350 K using the Nosé-Hoover thermostat for every molecule in the system. Although the shear softening effect by heating a viscoelastic fluid by shear field [14] is not treated in the simulation, we already succeeded in reproducing the saturation in the traction coefficient reported by experiments.

In order to explain all experimental phenomena, the heat transport within the film thickness under the experimental conditions may also be studied in future simulations.

4. Conclusions

All-atom MD simulations are used to calculate the effect of pressure under confinement and sliding. The limiting shear stress of the EHL molecular oil film is reproduced by the simulation. This phase transition is related to the suppression of the fluctuation in the molecular motion.

Acknowledgement

This work was partially supported by the Next Generation Super Computing Project, Nanoscience Program, Ministry of Education, Culture, Sports, Science and Technology, Japan. We also thank Prof. Dr. Shi-aki Hyodo, Dr. Shuzo Sanda and Prof. Dr. Yuichi Nakamura for useful discussions.

References

References

- [1] D. Dowson, G. Higginson (Eds.), *Elasto-Hydrodynamic Lubrication* (SI Edition), si edition Edition, International Series on Materials Science and Technology, Pergamon, 1977.
- [2] H. Washizu, T. Ohmori, Molecular dynamics simulations of elastohydrodynamic lubrication oil film, *Lubrication Sciences* 22 (2010) 323.
- [3] H. Washizu, S. Hyodo, S. Ohmori, N. Nishino, A. Suzuki, Macroscopic no-slip boundary condition confirmed in full atomistic simulation of oil film, *Tribology Online* 9 (2) (2014) 45–50.
- [4] S. Bair (Ed.), *High pressure rheology for quantitative elastohydrodynamics*, Elsevier, 2007.
- [5] K. Miyazaki, D. Reichman, R. Yamamoto, Supercooled liquids under shear: Theory and simulation, *Phys. Rev. E* 70 (011501).
- [6] W. D. Cornell, P. Cieplak, C. I. Bayly, I. Gould, K. M. Jr, D. Ferguson, D. Spellmeyer, T. Fox, J. Caldwell, P. Kollman., A second generation force field for the simulation of proteins and nucleic acids, *J. Am. Chem. Soc.* 117 (1995) 5179–5197.
- [7] S. Nose, A unified formulation of the constant-temperature molecular dynamics methods, *J. Chem. Phys.* 81 (1984) 511.
- [8] R. Khare, J. de Pablo, A. Yethiraj, Molecular simulation and continuum mechanics study of simple fluids in non-isothermal planar couette flows, *J. Chem. Phys.* 107(7) (1997) 2589–2596.
- [9] M. L. Greenfield, H. Ohtani, Packing of simulated friction modifier additives under confinement, *Langmuir* 21 (2005) 7568–7578.
- [10] M. Tuckerman, B. J. Berne, G. J. Martyna, Reversible multiple time scale molecular-dynamics, *J. Chem. Phys.* 97 (3) (1992) 1990.
- [11] P.W. Bridgman, Viscosities to 30,000 Kg/cm²: Further Rough Compressions to 40,000 Kg/cm², Especially Certain Liquids, *Proceedings of the American Academy of Arts and Sciences* (1949) 138.
- [12] P. Morawski, J.A.P. Coutinho, U. Domanska, High pressure (solid + liquid) equilibria of n-alkane mixtures: experimental results, correlation and prediction, *Fluid Phase Equilibria* 230 (2005) 72–80.

- [13] H. Eyring, Viscosity, plasticity, and diffusion as examples of absolute reaction rates, *J. Chem. Phys.* 4 (1936) 283.
- [14] H. Kobayashi, Y. Fujita, Mechanisms for three kinds of limiting shear stresses appearing in the traction modes of viscous, viscoelastic, and glassy states of lubricants, *J. Appl. Phys.* 115 (2014) 223509.

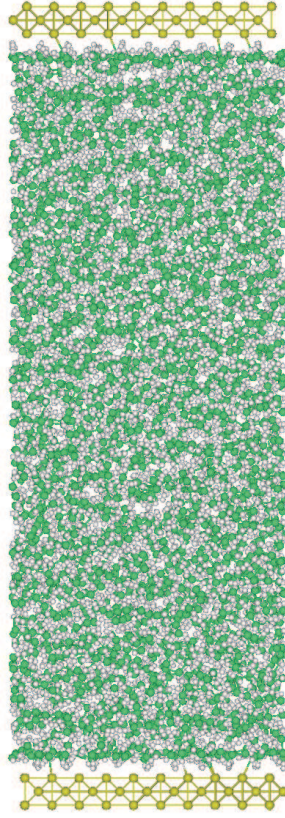


Figure 1: Snapshot of the molecular dynamics simulation of n-hexane fluid film at external pressures $p_{zz} = 8.0$ GPa.

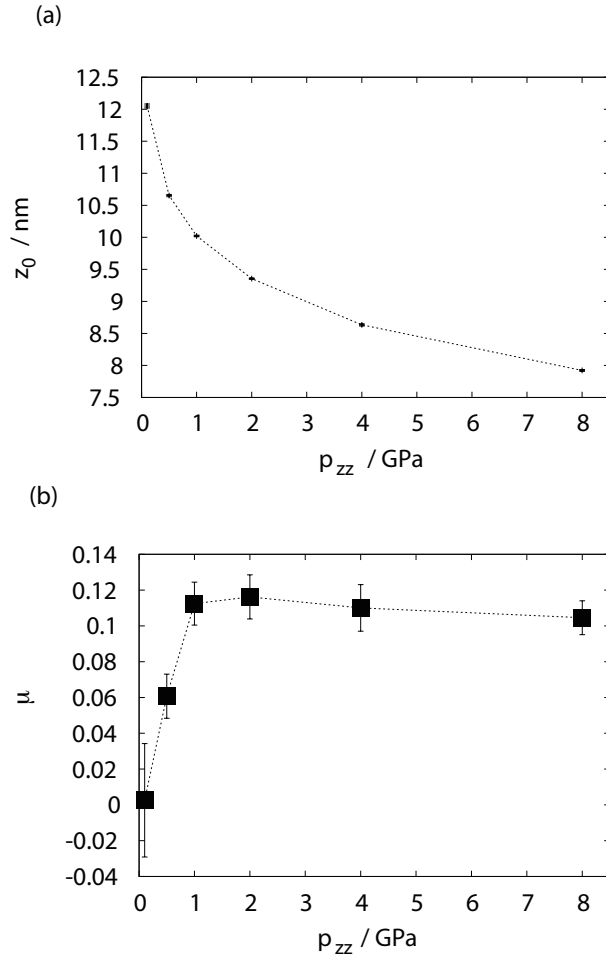


Figure 2: External pressure dependencies of (a) the film thickness and (b) the traction coefficient calculated from MD simulations.

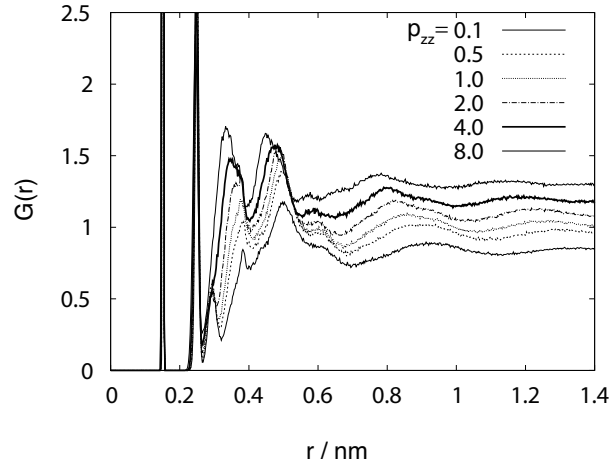


Figure 3: Radial distribution functions (RDFs) of carbon atoms $G(r)$ at various external pressures. All lines are normalized by the average concentration at $p_{zz} = 1.0$ GPa.

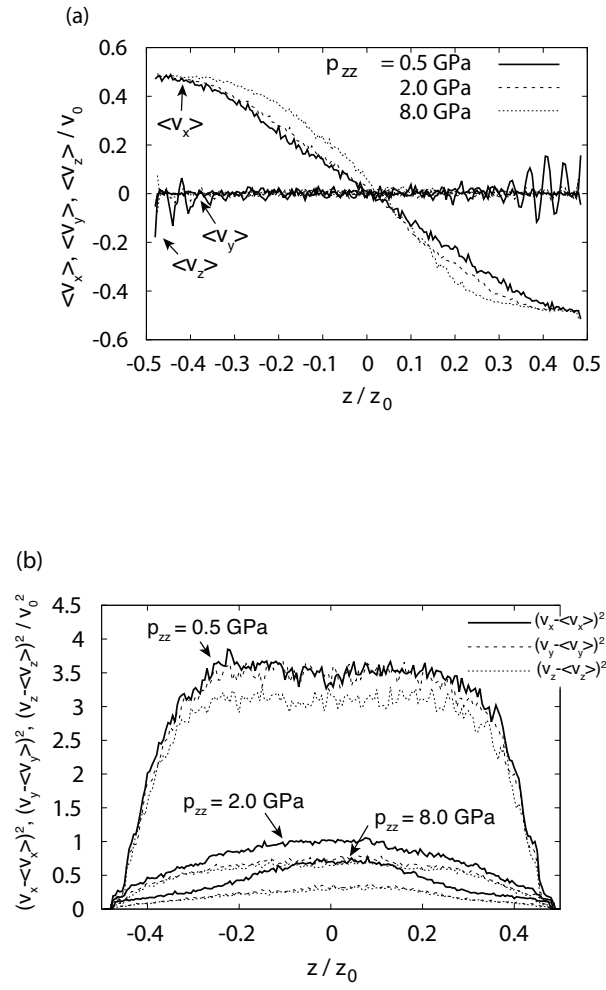


Figure 4: Profiles of (a) the velocities v_x , v_y , and v_z and (b) the velocity fluctuations $(v_x - \langle v_x \rangle)^2$, $(v_y - \langle v_y \rangle)^2$, and $(v_z - \langle v_z \rangle)^2$ at external pressures $p_{zz} = 0.5$, 2.0, and 8.0 GPa.

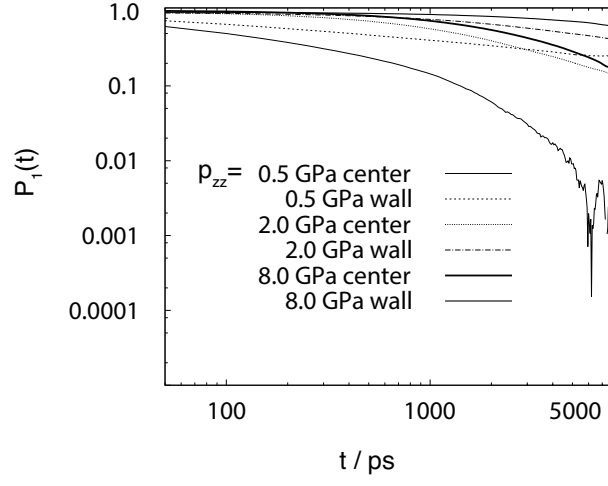


Figure 5: Variations in the segment correlation functions $P_1(t)$ at external pressures $p_{zz} = 0.5, 2.0$, and 8.0 GPa.